Pre-Steady-State Kinetic Studies of *Saccharomyces cerevisiae* MyristoylCoA:Protein *N*-Myristoyltransferase Mutants Identify Residues Involved in Catalysis†

Thalia A. Farazi,‡ Jill K. Manchester,‡ Gabriel Waksman,§ and Jeffrey I. Gordon*,‡

Departments of Molecular Biology and Pharmacology and of Biochemistry and Molecular Biophysics, Washington University School of Medicine, St. Louis, Missouri 63110

Received April 19, 2001; Revised Manuscript Received June 5, 2001

ABSTRACT: MyristoylCoA:protein *N*-myristoyltransferase (Nmt, EC 2.3.1.97), a member of the GCN5 acetyltransferase (GNAT) superfamily, is an essential eukaryotic enzyme that catalyzes covalent attachment of myristate (C14:0) to the N-terminal Gly of proteins involved in myriad cellular functions. The 2.5 Å resolution structure of a ternary complex of *Saccharomyces cerevisiae* Nmt1p with a bound substrate peptide (GLYASKLA) and nonhydrolyzable myristoylCoA analogue [Farazi, T. A., et al. (2001) *Biochemistry 40,* 6335] was used as the basis for a series of mutagenesis experiments designed to define the enzyme's catalytic mechanism. The kinetic properties of an F170A/L171A Nmt mutant are consistent with the proposal that their main chain amides, located in a β-bulge structure conserved among GNATs, function as an oxyanion hole to polarize the thioester carbonyl of bound myristoylCoA prior to subsequent nucleophilic attack. Removal of the two C-terminal residues (M454 and L455) produces a 300−400-fold reduction in the chemical transformation rate and converts the rate-limiting step from a step after the transformation to the transformation event itself. This finding is consistent with the main chain C-terminal carboxylate of L455 functioning as a catalytic base that abstracts a proton from the N-terminal Gly ammonium of the bound peptide to generate the nucleophilic amine. Mutating N169 and T205 in concert reduces the rate of the chemical transformation, supporting their role as components of an H-bonding network that facilitates attack of the Gly1 amine and stabilizes the tetrahedral intermediate.

MyristoylCoA:protein *N*-myristoyltransferase (Nmt),[1] a member of the GCN5-related *N*-acetyltransferase (GNAT) superfamily, catalyzes covalent attachment of myristate to the N-terminal Gly residue of eukaryotic proteins involved in diverse and important cellular activities (e.g., signal transduction and vesicular trafficking; reviewed in ref *1*). Typically, N-myristoylation is cotranslational and irreversible (*2*). To date, 19 Nmts have been identified from 15 eukaryotic species. Genetic studies have established that Nmt is an essential enzyme in *Saccharomyces cerevisiae* (*3*), in the two organisms that are the principal cause of systemic fungal infections in immunocompromised humans [*Candida albicans* and *Cryptococcus neoformans* (*4*, *5*)], in *Arabidopsis thaliana* (*6*), and in *Drosophila melanogaster* (*7*).

N-Myristoylproteins are associated with a variety of cellular membranes and are also cytosolic. Myristate promotes weak and reversible protein−membrane and protein−protein interactions. Typically, myristate does not act alone, but rather in concert with other mechanisms to regulate protein targeting and function. These other mechanisms are collectively termed "myristoyl-containing" switches. Examples include (i) myristoyl−electrostatic switches, where extra membrane binding affinity is provided through positively charged residues that interact with negatively charged membrane phospholipids, (ii) myristoyl−conformational switches, where exposure or sequestration of myristate occurs after ligand binding-induced changes in protein structure, and (iii) dual fatty acylation switches, where a second lipid modification (e.g., S-palmitoylation) provides additional membrane binding affinity (*1*).

Nmt can be distinguished from other GNAT family members on the basis of the remarkable diversity of its protein substrates. For example, the yeast genome encodes 71 known or putative Nmt1p substrates (∼1% of all proteins; *8*).

S. cerevisiae Nmt1p is the best studied of the known Nmts. This 455-residue monomeric enzyme has no known cofactor requirements. Its reaction mechanism is ordered bi-bi. MyristoylCoA binds first, followed by peptide. After the catalytic transfer of myristate, CoA and subsequently myristoylpeptide are released (*8*−*10*). Transient-state kinetic studies have disclosed that the rate-limiting step in the reaction mechanism occurs after chemical transformation (i.e., after conversion of the enzyme−substrate complex to the enzyme−product complex) (*11*).

The structure of a binary complex of Nmt1p with bound myristoylCoA has been determined to 2.2 Å resolution (*8*). A ternary complex of Nmt1p with a bound nonhydrolyzable myristoylCoA analogue [*S*-(2-oxo)pentadecylCoA] and an octapeptide substrate has also been defined to 2.5 Å

† This work was supported by NIH Grant AI38200. T.A.F. was supported in part by Medical Scientist Training Program Grant GM07200.

* To whom correspondence should be addressed: Department of Molecular Biology and Pharmacology, Washington University School of Medicine, Box 8103, 660 S. Euclid Ave., St. Louis, MO 63110. Phone: (314)362-7243. Fax: (314)362-7047. E-mail: jgordon@molecool.wustl.edu.

‡ Department of Molecular Biology and Pharmacology.

§ Department of Biochemistry and Molecular Biophysics.

[1] Abbreviations: Nmt, myristoylCoA:protein *N*-myristoyltransferase; GNAT, GCN5-related *N*-acetyltransferase.

10.1021/bi0107997 CCC: $20.00 © 2001 American Chemical Society
Published on Web 07/11/2001

resolution (*8*). The Nmt1p fold consists of a saddle-shaped β-sheet flanked on both faces by several helices. The fold has pseudo-2-fold symmetry: the N-terminal half of the protein forms the binding site for myristoylCoA, while the C-terminal half forms the bulk of the peptide binding site (Figure 1A). MyristoylCoA is bound in a bent conformation resembling a question mark, with bends located at pyrophosphate, at the C6−C7 group of pantetheine, and at C1 and the C5−C6 group of myristate (Figure 1A).

These structures suggested that the N-myristoylation reaction proceeds through a nucleophilic addition−elimination reaction where the nucleophilic N-terminal Gly amine of the peptide substrate attacks the polarized thioester carbonyl of myristoylCoA. Three elements in Nmt's active site were postulated to facilitate this reaction. An oxyanion hole, which could polarize the reactive carbonyl and accommodate the developing negative charge in the tetrahedral intermediate, appeared to be formed by the backbone amides of F170 and L171 (Figure 1B). The C-terminal carboxylate of L455, positioned within 2.9 Å of the N-terminal Gly nitrogen of the acceptor peptide, was postulated to function as the catalytic base that deprotonates the Gly ammonium to a nucleophilic amine (Figure 1C). The N-terminal Gly nitrogen in the ternary Nmt structure was positioned 6.3 Å from the polarized carbonyl. However, a 180 °C rotation along Ψ would reduce the distance to 4.3 Å and would place the amine along the reaction trajectory (*8*). Hydrogen bonding interactions between the Gly1 amine and Nmt residues N169 and T205 were postulated to act in concert to position the amine along this reaction trajectory and to facilitate the nucleophilic attack (Figure 1D).

In this report, we have performed steady-state and pre-steady-state analyses of site-directed Nmt mutants to test these structure-based hypotheses regarding the myristoyl transfer reaction.

MATERIALS AND METHODS

Site-Directed Mutagenesis. Site-directed mutagenesis of *S. cerevisiae* Nmt1p was performed using PCR and pBB376 (*12*). Four oligonucleotides were used to generate each mutant: two mutagenic primers (M1 and M2) with overlapping sequences on both strands and two flanking primers (F1 and R1). In the first step, two separate PCRs were performed to produce two fragments with overlapping sequences. The two fragments were then mixed, denatured, and annealed to obtain a template for a final PCR that uses only the F1 and R1 primers. A list of all oligonucleotides used for sequence overlap extension mutagenesis can be found at http://www.gordonlab.wustl.edu/farazi/nmt.

The PCR product was subcloned into pBB502, a derivative of pBB376 (*12*) but lacking codons specifying an N-terminal tag of six His residues. The ORF encoding each mutant Nmt was placed under the control of an isopropyl β-D-thiogalactopyranoside(IPTG)-inducible P_{tac} promoter. All *NMT1* ORFs were sequenced in their entirety to ensure that only the desired mutations were present. The following plasmids were used to express wild-type or mutant Nmts: pBB502 (wild-type), pBB435 (N169L), pBB431 (T205A), pBB438 (N169L/T205A), pBB436 (F170A/L171A), pBB439 (E167Q), and pBB441 (M454stop).

Purification of Nmts from E. coli. Cultures (9 L) of *E. coli* strain JM101 containing one of the plasmids listed above were incubated at 24 °C in LB medium containing 30 μg/mL streptomycin. Expression of wild-type or a mutant Nmt was induced with IPTG (100 μM), and the acyltransferase was purified to apparent homogeneity, free of thioesterase activity, as described in an earlier report (*13*). Each enzyme was dialyzed into storage buffer [50 mM *N*-(2-hydroxyethyl)-piperazine-*N*′-2-ethanesulfonic acid (pH 7.5), 1 mM DTT, and 15 mM EDTA], and the protein concentration was defined using a molar extinction coefficient of 63 163 M^{-1} cm^{-1} (at 280 nm; *11*).

Steady-State Nmt Assay. This assay allows continuous monitoring of CoA, the first product released by Nmt. It is a derivative of a recently described assay used for pre-steady-state kinetic studies of wild-type Nmt1p (*11*). In the new steady-state assay, CoA is detected by enzymatic coupling using succinylCoA synthetase (SCS), pyruvate kinase (PK), and lactate dehydrogenase (LDH) (Figure 2). A decrease in NADH fluorescence results from its conversion to NAD^+. The fluorescence reading is converted to CoA concentration using a panel of CoA standards. A buffer blank that included all reagents except the peptide substrate was always run in parallel.

The assay was validated as follows. Using wild-type Nmt1p, we established that the fluorescence change was substrate-dependent and linear as a function of incubation time (0−40 min). Moreover, the observed rate of the fluorescence change was linear with the amount of purified Nmt1p added (data not shown). The steady-state K_m and V_{max} for all coupling enzymes were determined using the Nmt1p assay conditions (described below). The V_{max} for all the coupling enzymes was found to be greater than the V_{max} for the Nmt1p-catalyzed reaction (Table 1). To ensure that the coupling enzymatic steps were faster than the rate of the Nmt1p reaction, we used the concentrations of coupling enzymes and their substrates that are listed below.

To perform the assay, purified wild-type or a mutant Nmt was added to 1 mL of a reaction mixture (final enzyme concentration of 10 nM) that also contained 50 mM Tris-succinate (pH 7.7), 5 mM $MgCl_2$, 0.5 mM DTT, 0.1 mM EDTA, 75 mM KCl, 500 μM phophoenolpyruvate, 100 μM GTP, 15 μM NADH, 10 μg/mL pig heart succinylCoA synthetase (specific activity of 0.01 unit/μg; obtained from Roche, Mannheim, Germany), 20 μg/mL rabbit muscle pyruvate kinase (0.2 unit/μg; Roche), and 2 μg/mL bovine heart lactate dehydrogenase (0.6 unit/μg; Sigma, St. Louis, MO). GTP was pretreated with epichlorohydrin triethanolamine cellulose to remove contaminating GDP. NADH fluorescence was measured (excitation at 355 nm and emission at 460 nm).

Steady-state kinetic assays were performed at 20 °C. K_m and k_{ss} were determined for each substrate at a saturating concentration of the nonvaried substrate (saturating is defined in this report as $\geq 6K_m$). Note that we use the term k_{ss} instead of k_{cat}, since k_{cat} does not correspond to the rate of Nmt1p's chemical transformation (*11*). For viscosity assays, sucrose was included at final concentrations of 10, 20, and 30%.

Pre-Steady-State Nmt Assays. This assay was performed as described by Farazi et al. (*11*). Two 30 μL reaction mixtures were assembled, one containing a purified thioesterase-free wild-type or a mutant Nmt (2 μM) and the other containing saturating concentrations of a purified octapeptide (Biomolecules Midwest, Waterloo, IL) in addition to myris-

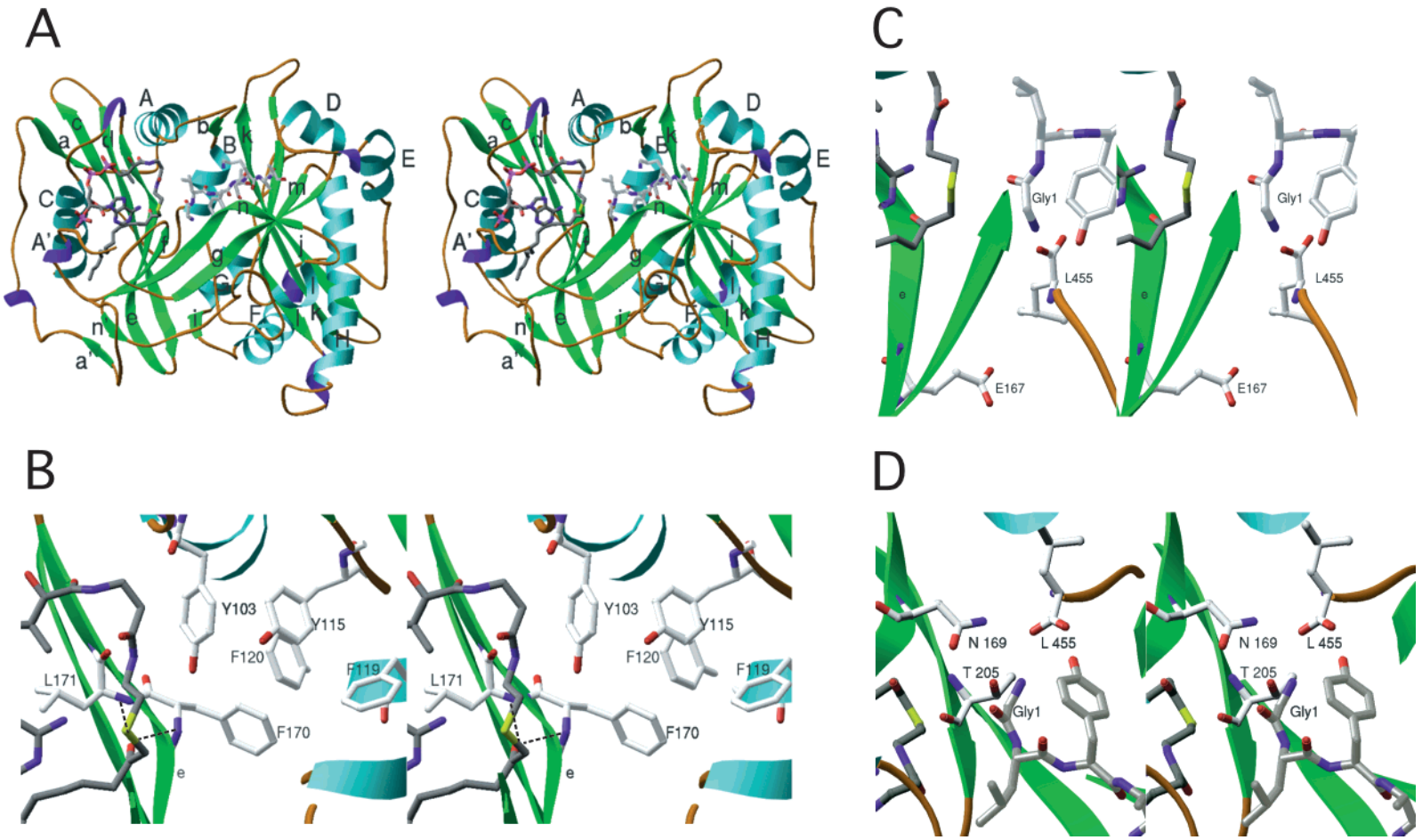

FIGURE 1: Structure of Nmt1p. (A) Stereoviews of a ribbon diagram from the 2.5 Å resolution structure of the ternary complex of Nmt1p with bound *S*-(2-oxo)pentadecylCoA and GLYASKLA. Secondary structure code: α-helices, light blue; 3_{10}-helices, deep blue; β-strands, green; and loops, amber. Atom color code: oxygen, red; phosphorus, pink; carbon, silver; nitrogen, purple; and sulfur, yellow. The carbon atoms of the ligands are dark gray. The nomenclature for helices and strands in Nmt is taken from Weston et al. (*29*). (B) The putative oxyanion hole, composed of the main chain amides of F170 and L171. These residues are positioned in a β-bulge located in strand e. Hydrogen bonds between the carbonyl of the myristoylCoA analogue and the main chain amides are indicated by dashed lines. (C) Locations of the main chain carboxylate of L455 and the side chain carboxylate of E167. (D) Relative positions of the N-terminal Gly1 of GLYASKLA, N169L, T205, and L455.

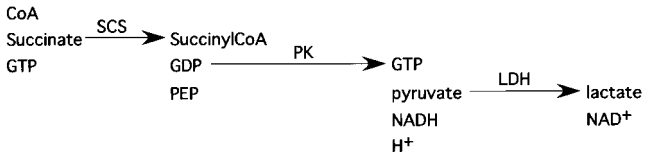

FIGURE 2: Method used for steady-state kinetic assays of wild-type and mutant Nmts. See the text for details: SCS, succinylCoA synthetase; PEP, phosphoenolpyruvate; PK, pyruvate kinase; LDH, lactate dehydrogenase.

Table 1: Validation of the Steady-State Nmt Assay[a]

enzyme	experimental value	literature value
lactate dehydrogenase (beef heart)	K_m(pyruvate) = 50 μM	30 μM
	K_m(NADH) = 3.3 μM	3 μM
	V_{max} = 817 s^{-1}	584 s^{-1}
pyruvate kinase (rabbit muscle)	K_m(PEP) = 40 μM	30 μM
	K_m(GDP) = 70 μM	280 μM
	V_{max} = 88 s^{-1}	112 s^{-1}
succinylCoA synthetase (pig heart)	K_m(GTP) = 8 μM	
	K_m(CoA) = 10 μM	10 μM
	K_m(succinate) = 50 μM	
	V_{max} = 8.2 s^{-1}	23.4 s^{-1}
Nmt1p	K_m(MyrCoA) = 1.4 μM	
	K_m(GAAPSKIV) = 0.9 μM	
	V_{max} = 0.3 s^{-1}	

[a] K_m and V_{max} for all enzymes used in the coupled assay were determined in Nmt assay buffer. Literature values are taken from ref *28*.

toylCoA (Sigma). Both reaction mixtures contained 10 mM Tris-HCl (pH 8.1), 5 mM $MgCl_2$, 0.5 mM DTT, and 0.1 mM EDTA. Following a 10 min pre-equilibration at 24 °C, the two samples were mixed using a Rapid Quenched-Flow apparatus (KinTek, Austin, TX). The reaction was quenched at various times after initiation (2 ms to 30 s) by adding 0.16 mL of 0.14 N perchloric acid. A sample with myristoylCoA but without peptide was used as a reference negative control.

Quenched samples were centrifuged at 12000*g* for 2 min at room temperature to pellet the precipitated protein. A 0.1 mL aliquot was removed and neutralized with 10 μL of a solution containing 1.03 M KOH, 0.55 M Tris-HCl (pH 8.1), and 2.2 μM *S*-(2-oxo)pentadecyl-CoA (*14*). The nonhydrolyzable myristoylCoA analogue was included to ensure there would be no residual Nmt1p activity during the subsequent CoA detection assay (*11*). All assays were performed in duplicate. The amount of CoA produced was plotted versus time and fit to the following equation:

$$[\mathrm{CoA}] = A(1 - e^{-k_b t}) + k_{ss} t \quad (1)$$

where A is the amplitude of the single exponential (burst phase), k_b is the burst rate, and k_{ss} is the steady-state rate. The kinetic parameters A, k_b, and k_{ss} were calculated using nonlinear least-squares analysis.

Equilibrium Fluorescence Measurements of MyristoylCoA Binding. The dissociation constant of wild-type Nmt1p and mutant Nmts for myristoylCoA was determined as described in ref *11*. The reaction mixture contained 200 nM Nmt, 20 mM HEPES (pH 7.5), 50 mM NaCl, and myristoylCoA (5−300 nM). The time course of fluorescence change was recorded, at increasing concentrations of myristoylCoA, using a PTI Photon Technology fluorimeter [excitation at 295 nm (2 nm slit) and emission at 330 nM (5 nm slit)]. The extent of tryptophan fluorescence quenching, Q_{obs}, was plotted as a function of the total substrate concentration. The titration data were fit to a one-site binding scheme using Scientist.

RESULTS

Before proceeding with the mutagenesis studies, we performed steady-state and pre-steady-state kinetic analysis to further characterize features of wild-type Nmt1p that could be audited in mutant derivatives. As noted in the introductory section, transient-state kinetic studies of Nmt1p revealed that a step after the chemical transformation is rate-limiting (*11*). However, these studies could not distinguish whether the rate-limiting step corresponds to diffusional product release or an isomerization step required for product dissociation. One method for elucidating the nature of the rate-determining step is to examine the effect of increasing viscosity on the steady-state kinetics of an enzyme's reaction (*15*). By increasing the viscosity of a solution with a microviscogen such as sucrose, the rates of diffusional steps are slowed, whereas unimolecular processes such as isomerization should be unaffected. Therefore, the effects of sucrose on the overall steady-state reaction rate (k_{ss}) were examined using two Nmt1p substrates: GAAPSKIV, corresponding to the N-terminus of *S. cerevisiae* Cnb1p (homologous to the regulatory component of mammalian calcineurin B; *16*), and GLYASKLA, derived from the N-terminus of *S. cerevisiae* ADP ribosylation factor 2 [*17*; note that the 2.5 Å resolution structure of Nmt1p with bound GLYASKLA and the nonhydrolyzable myristoylCoA analogue *S*-(2-oxo)pentadecylCoA had provided molecular insights about the interactions between this octapeptide substrate and the enzyme]. GNAAPARR was used as a control peptide, since pre-steady-state studies had revealed that in its presence the Nmt1p reaction is limited by the chemical transformation rate (data not shown).

In the absence of sucrose, the k_{ss} for Nmt1p was 0.3 ± 0.03 (GAAPSKIV), 0.5 ± 0.06 (GLYASKLA), and 0.004 ± 0.0015 s^{-1} (GNAAPARR). Adding up to 30% sucrose to the reaction mixture (~2.5-fold increase in relative viscosity) did not affect the overall rate of the reaction for any of the three substrates tested, suggesting that an isomerization step occurring after chemical transformation is rate-limiting.

We chose to assay the effects of site-directed mutagenesis of Nmt1p using both GLYASKLA and GAAPSKIV to assess the generality of the functional consequences of amino acid substitution or deletion. Table 2 presents the results of pre-steady-state and steady-state analysis of the wild-type enzyme in the presence of each peptide. GLYASKLA has a 7-fold higher burst rate (k_b) than GAAPSKIV, while their steady rates (k_{ss}) varied less than 2-fold (n = 3 independent experiments). The burst rates should correspond to the rate of the chemical transformation, since the reaction was performed using saturating concentrations of these two substrates.

Together, these kinetic studies allowed us to conclude that (i) a step after chemical transformation is rate-limiting for Nmt1p, (ii) the rate-limiting step likely reflects an isomerization (conformational change), and (iii) the rate of chemical transformation is 216-fold faster than the overall reaction rate in the case of GLYASKLA, and 53-fold greater with

Table 2: Steady and Pre-Steady-State Analysis of the Effects of Mutation of Residues Postulated To Be Involved in Catalysis[a]

	k_b (s^{-1})		k_{ss} (s^{-1})		K_m (μM)		K_d (nM)
Nmt	GLYASKLA	GAAPSKIV	GLYASKLA	GAAPSKIV	GLYASKLA	GAAPSKIV	myristoylCoA
wild-type	108	16	0.5	0.3	1.6	0.9	2.6
F170A/L171A	15	2	0.6	0.2	14	125	117
M454stop	0	0	0.37	0.04	3.6	1.25	5.6
E167Q	148	39	0.26	0.17	1.5	1	2.5
N169L	15	41	0.9	0.2	18.5	20	nd[b]
T205A	49	37	1.0	0.2	4.5	1.4	nd[b]
N169L/T205A	3.4	0.9	0.11	0.05	25	50	6.9

[a] Steady-state experiments to determine k_{ss} and K_m were performed with 10 nM Nmt and saturating concentrations of the nonvaried substrate ($\geq 6K_m$). Multiple-turnover pre-steady-state kinetic studies employed 1 μM Nmt and saturating amounts of the two substrates. [b] Not determined.

GAAPSKIV. Since both octapeptide substrates share the same reactive group, the observed difference in the rate of chemical transformation could reflect subtle differences in the positioning of their primary Gly amine group.

Mutagenesis of Residues Comprising the Oxyanion Hole (F170A/L171A) Affects Binding of Both Substrates and Reduces the Rate of Chemical Transformation. F170 and L171 of βe, postulated to comprise Nmt1p's oxyanion hole, are conserved among the orthologous Nmts. Their backbone amides appear to be responsible for polarization of the thioester carbonyl of bound myristoylCoA. To test this proposal directly, F170 and L171 were both mutated to Ala. We reasoned that a double mutation would destabilize the β-bulge containing these two amino acids by disrupting their interactions with neighboring residues, i.e., the parallel stacked $\pi-\pi$ interactions that occur between the aromatic ring of F170 and Y103, Y115, F119, and F120 (Figure 1B), as well as the contacts between L171 and I149, L186, and T183. [The X-ray structures of the binary myristoylCoA−Nmt1p complex and the ternary *S*-(2-oxo)pentadecylCoA−Nmt1p−GLYASKLA complex also reveal that the Cδ2 side chain atom of L171 is located $\leq$4 Å from several components of the bound acylCoA: C6 of adenine, C13 of pantetheine, and C4 of myristate.]

The steady-state rate (k_{ss}) of the F170A/L171A double mutant was similar to that of wild-type Nmt1p, using either GLYASKLA or GAAPSKIV as the substrate. Viscosity experiments revealed that the k_{ss} for the F170A/L171A mutant was unchanged upon addition of 30% sucrose. Subsequent pre-steady-state kinetic studies disclosed a burst in product formation (Figure 3), but the burst rate (k_b) was 7−8-fold lower than the wild-type rate when assayed using GAAPSKIV and GLYASKLA (Table 2).

Reductions in k_b could occur as a result of a reduced level of polarization of the thioester carbonyl of myristoylCoA, or malpositioning of myristoylCoA within its binding site. In addition, the *S*-(2-oxo)pentadecylCoA−Nmt1p−GLYASKLA ternary complex structure had indicated that Gly1 and the Leu2 side chain of GLYASKLA interact with the pantetheine moiety of CoA that forms an integral part of the peptide binding site. These contacts generate a 90° bend in the peptide backbone, turning it away from the myristoylCoA analogue and toward a peptide-binding groove (Figure 1A). Thus, if the double mutant results in malpositioning of myristoylCoA in its binding site, the positioning of GLYASKLA could also be affected.

The effect of the mutations on substrate binding was investigated as follows. Equilibrium fluorescence quenching experiments disclosed that the K_d for myristoylCoA was 45-fold higher for the double mutant than for wild-type Nmt1p (117 vs 2.6 nM, respectively; Table 2). Steady-state kinetic studies revealed a 48-fold increase in K_i for *S*-(2-oxo)-pentadecylCoA (1200 vs 25 nM). The double mutation also affected peptide binding. There were significant increases in K_m for both octapeptide substrates (9-fold for GLYASKLA and 139-fold for GAAPSKIV; see Table 2). There was a 75-fold increase in K_i (from 60 to 4500 nM) for SC-58272, a dipeptide competitive inhibitor derived from GLYASKLA. [SC-58272 retains the critical Ser5 and Lys6 recognition elements, but the N-terminal GLYA is replaced with a 2-methylimidizole plus a rigidified carbon linker [*p*-(2-methylimidazole-*N*-butyl)phenylacetyl], and the C-terminal Leu-Ser with cyclohexylethyl (*18*).]

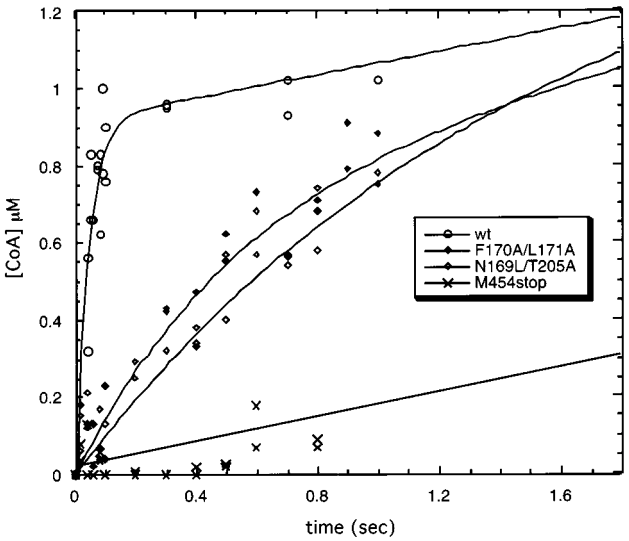

FIGURE 3: Multiple-turnover pre-steady-state kinetic analysis of wild-type and mutant Nmts. Assays were performed at 24 °C. [Nmt1p] = 1 μM. [MyristoylCoA] = 20 μM. [GAAPSKIV] = 20−1000 μM (i.e., at least 6K_m for wild-type or mutant Nmt). The level of CoA product formation is plotted as a function of reaction time. The data were fit using eq 1 described in Materials and Methods to define the burst rate (k_b). The k_b for wild-type Nmt1p with GAAPSKIV is 16 ± 2.5 s^{-1} (n = 6 experiments).

Together, these studies led us to conclude that like wild-type Nmt1p, the rate limiting step of the F170A/L171A mutant occurs after the chemical transformation. The double mutant produces an order of magnitude reduction in the burst rate that can be explained by malpositioning of the reactive groups of myristoylCoA in the oxyanion hole, leading to less efficient polarization of the thioester carbonyl. Given the contribution of the CoA pantetheine group to the peptide binding site, malpositioning of myristoylCoA also affects interactions between the enzyme and its second substrate.

Truncation of Two C-Terminal Residues Dramatically Reduces the Chemical Transformation Rate and Changes the Rate-Limiting Step in the Reaction. To test the postulate that the C-terminal main chain carboxylate of L455 functions as the catalytic base, a M454Stop mutant lacking the two C-terminal residues of Nmt1p was generated. Our reasoning for generating M454Stop was based on the following considerations. Inspection of the ternary structure indicated that truncating the C-terminus by one residue would position the newly created C-terminal main chain carboxylate only ~5 Å away from the Gly1 nitrogen of GLYASKLA, while a two-residue truncation would position this carboxylate ~8 Å away. Moreover, since the C-terminus of Nmt1p is located in the core of the protein (Figure 1A,C,D), it appeared to be unlikely that the Val453 carboxylate in the M454Stop mutant would be able to reposition itself close to the Gly1 nitrogen.

Steady-state kinetic studies of the purified M454Stop mutant revealed a k_{ss} similar to that of wild-type Nmt1p when GLYASKLA was used as the substrate, and an 8-fold reduction with GAAPSKIV (Table 2). The K_d for myristoylCoA, the K_i for *S*-(2-oxo)pentadecylCoA, and the K_m values for GLYASKLA and GAAPSKIV were not appreciably different for M454Stop and wild-type Nmt1p (Table 2 and data not shown).

Pre-steady-state studies disclosed that the C-terminal truncation changes the rate-limiting step for the myristoylation reaction. The burst phase observed with the wild-type enzyme is completely abolished for M454Stop using GLYASKLA or GAAPSKIV at concentrations $>6K_m$. The absence of a burst (Figure 3 and Table 2) indicates that chemical transformation is the rate-limiting step for this mutant. A viscosity study of M454stop did not show any effect on the overall reaction rate with 30% sucrose, consistent with chemical transformation being rate-limiting. To estimate the fold reduction in the rate of chemical transformation, the k_b of wild-type Nmt1p was divided by the k_{ss} for the mutant. The results reveal a 292-fold decrease for GLYASKLA and a 400-fold reduction for GAAPSKIV.

These findings support the postulate that the C-terminal main chain carboxylate of L455 functions as a catalytic base to deprotonate the Gly1 ammonium to the nucleophilic amine. The only other carboxylate positioned within 8 Å of the Gly1 nitrogen in the *S*-(2-oxo)pentadecylCoA−Nmt1p−GLYASKLA ternary complex structure is the side chain of E167 (Figure 1C). This Glu is highly conserved in orthologous Nmts. Moreover, as noted in the Discussion below, other GNAT family members use the side chain carboxylate of a comparably positioned Glu residue as their catalytic base.

An E167Q mutant was constructed to examine the role of the side chain carboxylate in catalysis. The results revealed that the burst rate of this mutant was slightly greater than that of the wild type, that its k_{ss} differed <2-fold from that of Nmt1p, and that the steady-state rate was not affected by 30% sucrose. (Table 1 and data not shown.) These findings establish that the side chain carboxylate of E167 is not needed for chemical transformation.

N169L/T205A Reduces the Chemical Transformation Rate. As noted above, the ternary structure suggested that the Oδ of N169 plus the side chain hydroxyl (Oγ) and main chain carbonyl of T205 contribute to an H-bonding network that involves the Gly1 nitrogen of GLYASKLA (Figure 1D). These two residues are absolutely conserved in all known orthologous Nmts. Three Nmt mutants were generated to test the postulate that this network is important in catalysis: N169L, T205A, and the double mutant N169L/T205A. The k_{ss} of the N169L and T205A single mutants was similar to that of wild-type Nmt1p, and was 5−6-fold lower with the N169L/T205A double mutant, as assayed with both octapeptide substrates (Table 2). A viscosity study of all three mutants did not result in any effects on their overall reaction rates at sucrose concentrations up to 30% (data not shown). The N169L/T205A mutant had a K_d for myristoylCoA that was within 3-fold of that of the wild type (Table 2). K_m values for GLYASKLA and GAAPSKIV varied ≤3-fold with T205A compared to that of Nmt1p, but were increased 12- and 22-fold with N169L and 16- and 56-fold with N169L/T205A, respectively.

Pre-steady-state kinetic studies using saturating concentrations of substrates revealed 2−7-fold changes in k_b for the single mutants. The double mutant produced 18−32-fold reductions in the burst rate (Table 2). These results establish that the H-bonding network contributed by both N169 and T205 facilitates catalysis.

The ternary complex structure reveals only three nucleophilic residues located within 10 Å of the myristoylCoA thioester carbonyl: N169, T205, and Y103 (Figure 1B,D). All three residues are absolutely conserved among the known Nmts. Our findings provide evidence that N169 and T205 are important but not essential for catalysis, indicating that the reaction mechanism does not proceed through an acyl−enzyme intermediate that involves these residues. In addition, the overall reaction rate for a Y103F mutant was indistinguishable from that of the wild type (data not shown).

Mutagenesis of GLYASKLA. As noted in the introductory section, Nmt1p acylates a large repertoire of yeast proteins, perhaps as many as 1% of all cellular proteins. In vitro assays of >100 synthetic peptides representing derivatives of the N-terminal sequences of known N-myristoylproteins have shown that the enzyme is able to recognize and accommodate a variety of residues beyond the absolutely required Gly1 (*19*). Figure 4 summarizes salient molecular details of the interactions between GLYASKLA and Nmt1p provided by the 2.5 Å structure of the *S*-(2-oxo)pentadecylCoA−Nmt1p−GLYASKLA ternary complex. Leu2 in GLYASKLA is positioned over the aromatic side chains of Y103 and F113, and is surrounded on one side by V104, F111, and F334, and on the other side by the aliphatic chain of E105, and C4−C7 of pantetheine (Figure 4A). Tyr3 in GLYASKLA interacts with an aromatic cluster consisting of Y219, Y330, and Y349, in addition to L420 (Figure 4B). Ala4 is located in a large hydrophobic/aromatic pocket containing F111, F113, F234, F334, I347, and V395 (Figure 4C). Ser is strongly preferred at position 5 (37 of 71 known or putative yeast Nmt1p substrates). The Ser hydroxyl H-bonds to H221 and the backbone amides of G418 and D417 (Figure 4D). The ϵ-amino group of Lys6 H-bonds to the side chain of D417, while its aliphatic portion is surrounded by the side chains of F111 and F234 (Figure 4D). Leu7 and Ala8 make very few contacts.

The pre-steady-state kinetic analyses of the Nmt mutants described above examined how different elements of the enzyme contributed to catalysis. We performed a final series of "mutagenesis" experiments designed to define the extent to which residues at positions 2, 3, 5, and 6 of GLYASKLA

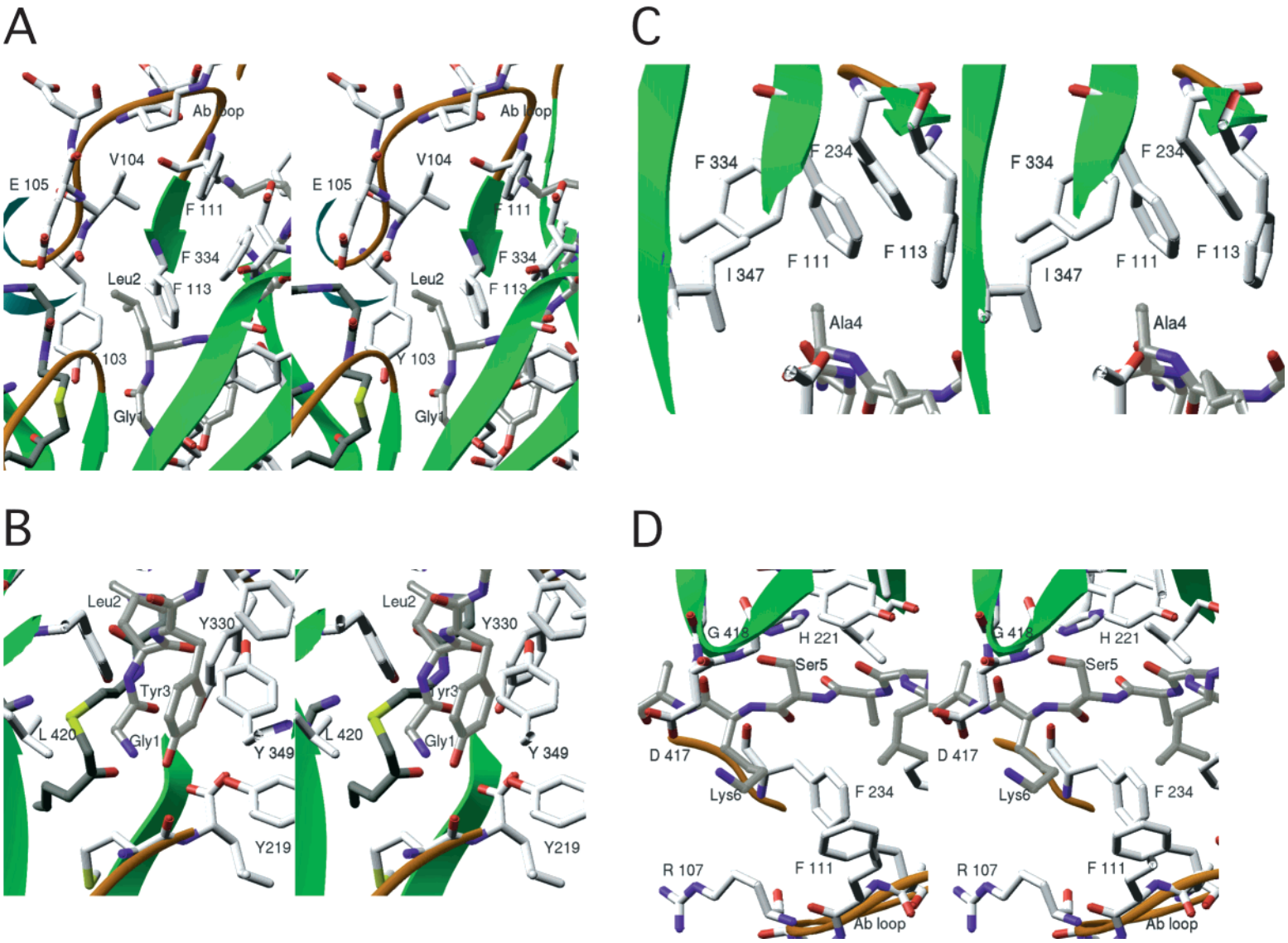

FIGURE 4: Features of the interaction between GLYASKLA and the peptide binding site of Nmt1p. The interactions that are shown are from the 2.5 Å structure of the *S*-(2-oxo)pentadecylCoA−Nmt1p−GLYASKLA ternary complex (*8*).

Table 3: Kinetic Characterization of Substrates Derived from Ala Scanning Mutagenesis of GLYASKLA[a]

substrate	k_b (s^{-1})	k_{ss} (s^{-1})	K_m (μM)
GLYASKLA	108	0.5	1.6
G**A**YASKLA	9	0.05	0.3
GL**A**ASKLA	90	0.08	0.4
GLYA**A**KLA	6	0.1	15
GLYAS**A**LA	8	0.05	23
GLYASK**A**A	19	0.8	6

[a] Multiple-turnover pre-steady-state kinetic studies were performed using 1 μM wild-type Nmt1p and saturating concentrations of substrates. Steady-state experiments to determine k_{ss} and K_m were performed using 20 μM myristoylCoA and 10 nM Nmt. Note that Ala substitution for Gly1 produced a peptide (ALYASKLA) that was not a substrate (K_i = 140 μM; competitive vs GLYASKLA).

contribute to proper placement of the Gly1 nitrogen in the active site. A panel of GLYASKLA derivatives with single Ala substitutions at these positions was produced. Pre-steady-state analysis, performed at saturating substrate concentrations ($\geq 6K_m$), indicated that Ala substitution for Leu2, Ser5, or Lys6 produced a 12−18-fold reduction in the burst rate (Table 3). In contrast, mutagenesis of Tyr3 had minimal effects on k_b (<2-fold difference compared to that of the "wild-type" peptide). The dispensability of Tyr3 is interesting in light of the ternary complex structure showing the Gly1 ammonium/amine H-bonded to the C-terminal L455 carboxylate. In this conformer, the Tyr3 hydroxyl is also within H-bonding distance (3.0 Å) of the Gly1 nitrogen (Figures 1D and 4B). The similar burst rates obtained with GL**Y**ASKLA and GL**A**ASKLA indicate that the Tyr hydroxyl does not facilitate deprotonation of the Gly1 ammonium.

The reactive group in Nmt1p substrates is invariant, i.e., a nucleophilic amine from the N-terminal Gly residue. The GLYASKLA mutagenesis results emphasize that differences in the efficiency of N-myristoylation of various cellular proteins may arise in part because of differences in the presentation of the Gly nitrogen dictated by interactions between residues 2, 5, and 6 of substrates and elements in the enzyme's peptide binding site.

DISCUSSION

In this report, we describe the results of a series of mutagenesis studies of *S. cerevisiae* Nmt1p designed to test a proposed catalytic mechanism inferred from the X-ray structure of the enzyme. The key findings are as follows. First, steady-state and pre-steady-state kinetic analyses of an F170A/L171A Nmt mutant indicate that the main chain amides of F170 and L171 function as an oxyanion hole which polarizes the thioester carbonyl of bound myristoylCoA prior to subsequent nucleophilic attack by the N-terminal Gly1 amine of a substrate peptide. The pantetheine moiety of CoA forms a part of Nmt's peptide binding site. The kinetic features of the double mutant also emphasize the contributions of the oxyanion hole to proper positioning of both myristoylCoA and peptide substrates. Second, removal of the C-terminal two residues of Nmt1p (M454 and L455) converts the rate-limiting step of the enzyme from a step after chemical transformation to the chemical transformation itself. This finding is consistent with the main chain C-terminal carboxylate (L455) functioning as a catalytic base that abstracts a proton from the N-terminal Gly ammonium of bound peptide substrates. The M454stop mutant exhibits a 300-400-fold reduction in the transformation rate, indicating the extent to which this catalytic base facilitates the nucleophilic addition−elimination reaction. Third, mutating N169 and T205, in concert, reduces the rate of chemical transformation, lending credence to their role as components of an H-bonding network that promotes attack of the nucleophilic amine and stabilizes the tetrahedral intermediate.

Current Understanding of the Nmt Reaction Derived from Structural and Kinetic Studies of Wild-Type and Mutant Enzymes

Conformational Changes Associated with Substrate Acquisition. Binding of myristoylCoA induces two important conformational changes in the apoenzyme: (i) a 3_{10}-helix (A′ in Figure 1A) is generated from the disordered N-terminus, and (ii) a loop connecting helix A and strand b (Ab loop; Figures 1A,4A) adopts a conformation that opens a portion of the peptide binding site. These conformational changes complete formation of the myristoylCoA binding site and allow acquisition of peptide. Once peptide is acquired, the Ab loop undergoes additional conformational changes that "close the lid" over the peptide binding site.

Nucleophilic Addition−Elimination Reaction. Figure 5 presents two conformers for the N-terminal Gly of the bound peptide substrate. One conformer, defined in the ternary complex structure, links the Gly1 ammonium/amine to the C-terminal carboxylate for deprotonation (Figure 5A). Another conformer forms after a rotation of the amine around Ψ, and is stabilized by additional H-bonds involving the side chain amide of N169, and the side chain hydroxyl and main chain carbonyl of T205 (Figure 5B). This H-bond network not only permits the neutral glycine nitrogen to approach the carbonyl group along the antibonding orbital axis for nucleophilic attack of the polarized myristoylCoA thioester carbonyl, but also stabilizes the developing tetrahedral intermediate (Figure 5C).

Product Release. Subsequent collapse of the tetrahedral intermediate leads to extrusion of CoA. During this process, the Gly1 amine needs to be deprotonated, while the thiolate leaving group needs to be protonated. In the scheme presented in Figure 5C, this occurs through proton exchange between these two groups. The thiolate leaving group is stabilized by the N6 amine of the CoA adenine (the S−N distance is 3.1 Å in the ternary structure). This intramolecular stabilization mechanism is economical and accounts for the bent conformation of CoA. Moreover, in this scheme the departing CoA would be globular and its compact size should facilitate diffusion from the active site.

Pre-steady-state kinetic studies reveal that a step after chemical transformation is rate-limiting for the Nmt1p reaction. Moreover, the results of measuring enzymatic rates in the presence of increasing buffer microviscosity indicate that an isomerization occurring after the chemical transformation is the likely rate-limiting step. We propose that this isomerization is the reverse of the conformational changes that occur upon myristoylCoA binding, i.e., that it involves disordering of the N-terminal 3_{10}-helix A′ and alteration of the Ab loop conformation.

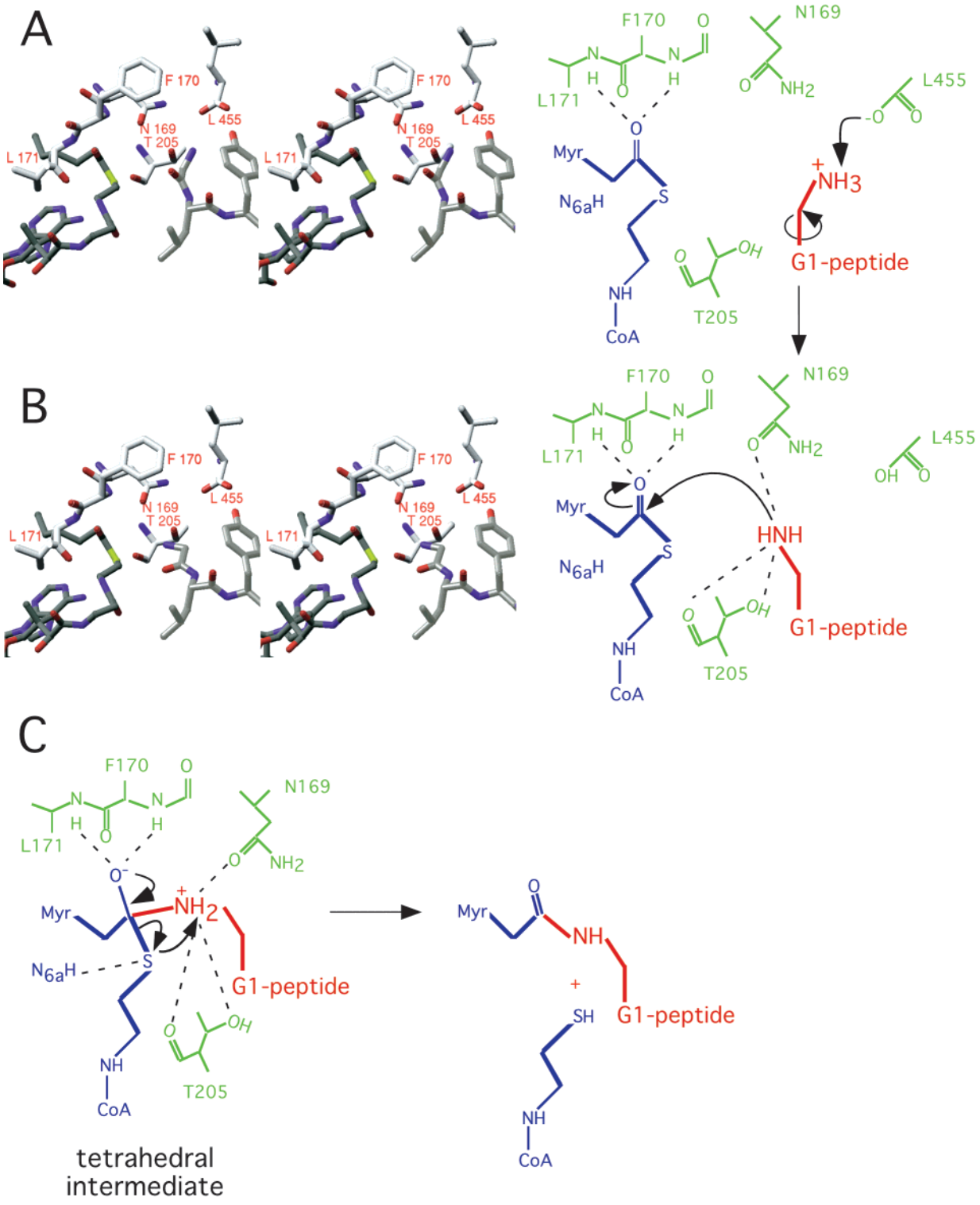

FIGURE 5: Proposed catalytic mechanism. (A) Conformer 1 is taken from the ternary structure of Nmt1p with bound *S*-(2-oxo)pentadecylCoA and GLYASKLA. (B) Conformer 2 is consistent with the mutagenesis studies. Conformer 2 is proposed to form after rotation of the Gly1 amine around Ψ, and is stabilized by additional H-bonds involving N169 and T205. The H-bond network promotes nucleophilic attack on the myristoylCoA thioester carbonyl, and stabilizes the developing tetrahedral intermediate (C).

Comparison with Other GNAT Family Members

Each of the symmetry-related halves of Nmt is topologically equivalent to the monomer core structure of GNAT superfamily members. All family members catalyze the transfer of an acyl group from CoA to a primary amino group. Structural and/or kinetic analyses of serotonin *N*-acetyltransferase (AANAT) and histone *N*-acetyltransferases from three species (human p300/CBP-associating factor, *Tetrahymena* GCN5, and *S. cerevisiae* Gcn5p; *20*−*25*) indicate that each of these enzymes follows an ordered reaction mechanism. The catalytic mechanism in each case involves direct nucleophilic attack of a primary amine on the thioester carbonyl of a bound acylCoA. This attack appears to be aided by polarization of the carbonyl by an

oxyanion hole formed by main chain amides of a conserved β-bulge, and by a catalytic base. In the yeast Gcn5p, the side chain of E173 in β-strand 4 functions as the catalytic base, exerting its effects through an ordered water; an E173Q Gcn5p mutant exhibits a 320-fold reduction in its steady-state rate compared to that of the wild type (*25*). In Esa1p, the catalytic subunit of the *S. cerevisiae* NuA4 histone acetylase, the side chain of E338 located in β-strand 10 appears to function as the catalytic base (*26*). Superimposition of the structures confirmed that the side chain carboxylates of these glutamates occupy a position in the active site comparable to that of the main chain carboxylate of L455 in Nmt1p (data not shown).

The rate-limiting step is known only for a few GNAT family members. In the case of AANAT, it appears to be diffusional release of product (*27*), while for human p300/CBP-associating factor, it is the chemical transformation step itself (*22*, *23*).

Manipulating Protein N-Myristoylation

Our studies of Nmt underscore the importance of further defining the details of its rate-limiting step. This will likely require additional types of kinetic analyses as well as structural (e.g., NMR) approaches for characterizing protein dynamics. Future efforts to manipulate protein N-myristoylation in vivo should be aided by this information, since compounds that interfere with the steps involved in product release may be very effective Nmt inhibitors. As noted above, the pantetheine moiety of myristoylCoA forms an integral part of the enzyme's peptide binding site. Bi-substrate analogues that exploit the shared specificity of orthologous Nmts for myristoylCoA *and* their differences in peptide recognition may also be effective inhibitors. In addition, it may be highly advantageous to attempt to incorporate features into these analogues that affect the conformation and/or dynamics of the Ab loop, given the proposed role of this loop in peptide binding and product release.

ACKNOWLEDGMENT

We thank Timothy Lohman and members of his lab for access to their quench flow apparatus.

REFERENCES

1. Bhatnagar, R. S., Ashrafi, K., Futterer, K., Waksman, G., and Gordon, J. I. (2000) in *The Enzymes: Protein Lipidation* (Tamanoi, F., and Sigman, D. S., Eds.) pp 241−290, Academic Press, San Diego.
2. Wolven, A., Okamura, H., Rosenblatt, Y., and Resh, M. D. (1997) *Mol. Biol. Cell 8*, 1159−1173.
3. Duronio, R. J., Towler, D. A., Heuckeroth, R. O., and Gordon, J. I. (1989) *Science 243*, 796−800.
4. Weinberg, R. A., McWherter, C. A., Freeman, S. K., Wood, D. C., Gordon, J. I., and Lee, S. C. (1995) *Mol. Microbiol. 16*, 241−250.
5. Lodge, J. K., Jackson-Machelski, E., Toffaletti, D. L., Perfect, J. R., and Gordon, J. I. (1994) *Proc. Natl. Acad. Sci. U.S.A. 91*, 12008−12012.
6. Qi, Q., Rajala, R. V., Anderson, W., Jiang, C., Rozwadowski, K., Selvaraj, G., Sharma, R., and Datla, R. (2000) *J. Biol. Chem. 275*, 9673−9683.
7. Ntwasa, M., Aapies, S., Schiffmann, D. A., and Gay, N. J. (2001) *Exp. Cell Res. 262*, 134−144.
8. Farazi, T. A., Waksman, G., and Gordon, J. I. (2001) *Biochemistry 40*, 6335−6343.
9. Rudnick, D. A., McWherter, C. A., Rocque, W. J., Lennon, P. J., Getman, D. P., and Gordon, J. I. (1991) *J. Biol. Chem. 266*, 9732−9739.
10. Bhatnagar, R. S., Schall, O. F., Jackson-Machelski, E., Sikorski, J. A., Devadas, B., Gokel, G. W., and Gordon, J. I. (1997) *Biochemistry 36*, 6700−6708.
11. Farazi, T. A., Manchester, J. K., and Gordon, J. I. (2000) *Biochemistry 39*, 15807−15816.
12. Zhang, L., Jackson-Machelski, E., and Gordon, J. I. (1996) *J. Biol. Chem. 271*, 33131−33140.
13. Bhatnagar, R. S., Futterer, K., Farazi, T. A., Korolev, S., Murray, C. L., Jackson-Machelski, E., Gokel, G. W., Gordon, J. I., and Waksman, G. (1998) *Nat. Struct. Biol. 5*, 1091−1097.
14. Paige, L. A., Zheng, G. Q., DeFrees, S. A., Cassady, J. M., and Geahlen, R. L. (1989) *J. Med. Chem. 32*, 1665−1667.
15. Blacklow, S. C., Raines, R. T., Lim, W. A., Zamore, P. D., and Knowles, J. R. (1988) *Biochemistry 27*, 1158−1167.
16. Cyert, M. S., and Thorner, J. (1992) *Mol. Cell. Biol. 12*, 3460−3469.
17. Stearns, T., Kahn, R. A., Botstein, D., and Hoyt, M. A. (1990) *Mol. Cell. Biol. 10*, 6690−6699.
18. Devadas, B., Zupec, M. E., Freeman, S. K., Brown, D. L., Nagarajan, S., Sikorski, J. A., McWherter, C. A., Getman, D. P., and Gordon, J. I. (1995) *J. Med. Chem. 38*, 1837−1840.
19. Towler, D. A., Gordon, J. I., Adams, S. P., and Glaser, L. (1988) *Annu. Rev. Biochem. 57*, 69−99.
20. Hickman, A. B., Namboodiri, M. A., Klein, D. C., and Dyda, F. (1999) *Cell 97*, 361−369.
21. De Angelis, J., Gastel, J., Klein, D. C., and Cole, P. A. (1998) *J. Biol. Chem. 273*, 3045−3050.
22. Lau, O. D., Courtney, A. D., Vassilev, A., Marzilli, L. A., Cotter, R. J., Nakatani, Y., and Cole, P. A. (2000) *J. Biol. Chem. 275*, 21953−21959.
23. Tanner, K. G., Langer, M. R., and Denu, J. M. (2000) *Biochemistry 39*, 11961−11969.
24. Rojas, J. R., Trievel, R. C., Zhou, J., Mo, Y., Li, X., Berger, S. L., Allis, C. D., and Marmorstein, R. (1999) *Nature 401*, 93−98.
25. Tanner, K. G., Trievel, R. C., Kuo, M. H., Howard, R. M., Berger, S. L., Allis, C. D., Marmorstein, R., and Denu, J. M. (1999) *J. Biol. Chem. 274*, 18157−18160.
26. Yan, Y., Barlev, N. A., Haley, R. H., Berger, S. L., and Marmorstein, R. (2000) *Mol. Cell 6*, 1195−1205.
27. Khalil, E. M., De Angelis, J., and Cole, P. A. (1998) *J. Biol. Chem. 273*, 30321−30327.
28. Passonneau, J. V., and Lowry, O. H. (1993) *Enzymatic Analysis*, Humana Press, Totowa, NJ.
29. Weston, S. A., Camble, R., Colls, J., Rosenbrock, G., Taylor, I., Egerton, M., Tucker, A. D., Tunnicliffe, A., Mistry, A., Mancia, F., de la Fortelle, E., Irwin, J., Bricogne, G., and Pauptit, R. A. (1998) *Nat. Struct. Biol. 5*, 213−221.

BI0107997